

## Low-temperature high-pressure preparation of transparent nanocrystalline $\text{MgAl}_2\text{O}_4$ ceramics

T. C. Lu, X. H. Chang, J. Q. Qi, and X. J. Luo

*Department of Physics, Sichuan University, Chengdu 610064, People's Republic of China; Key Laboratory of Radiation Physics and Technology, Sichuan University, Chengdu 610064, People's Republic of China; and International Center for Material Physics, Chinese Academy of Sciences, Shenyang 110015, People's Republic of China*

Q. M. Wei, S. Zhu, K. Sun, J. Lian, and L. M. Wang<sup>a)</sup>

*Department of Nuclear Engineering and Radiological Sciences, University of Michigan, Ann Arbor, Michigan 48109 and Department of Materials Science and Engineering, University of Michigan, Ann Arbor, Michigan 48109*

(Received 6 January 2006; accepted 12 April 2006; published online 26 May 2006)

Transparent  $\text{MgAl}_2\text{O}_4$  spinel nanoceramics have been sintered at relatively low-temperature (500–700 °C) under high pressure (2–5 GPa) using a hydrostatic press with high-temperature-calcined nanopowders. The morphology, nanostructure, optical property, and density of ceramics were analyzed by scanning electron microscopy, transmission electron microscopy, UV-VIS-IR transmission spectrum, and Archimedes draining method. The average grain size (<100 nm for all samples sintered) depends on the sintering pressure and temperature. The nanoceramics are highly transparent even though their relative densities are all less than 99%, due to the low or negligible light scattering from the nanosized grains and pores. © 2006 American Institute of Physics. [DOI: 10.1063/1.2207571]

Transparent  $\text{MgAl}_2\text{O}_4$  spinel ceramic has been considered as an important optical material due to its high melting point, good mechanical strength, high resistance against chemical attack, and excellent optical properties.<sup>1–3</sup> It has attracted a growing interest from both defense and civil industries. At present, the ceramic can be produced using hot pressing, vacuum sintering/hot isostatic pressing, or hot pressing/hot isostatic pressing.<sup>3–6</sup> The sintering temperature is usually above 1700 °C. However, transparency of the ceramics is found to depend, to a certain extent, on the pressure in the sintering process besides on the sintering temperature. Gallas *et al.*<sup>7,8</sup> studied the high-pressure compaction of nanosize powders using a diamond anvil high-pressure cell, and obtained translucent  $\gamma\text{-Al}_2\text{O}_3$  sample with a density just reached 90% of full density after a subsequent heat treatment at 800 °C that did not cause significant grain growth. The high-pressure compaction was independent of sintering in their work. One problem with transparent ceramics that has been gradually realized for actual applications is its poor mechanical property, i.e., brittleness. However, as for the transparent ceramic, the traditional toughening methods cannot be used since it decreases the transparency of the ceramic. Nanoceramic materials have many processing and property advantages over conventional coarse grained alternatives including the improved mechanical property.<sup>9</sup> In recent years, there has been an increasing interest in the synthesis of nanocrystalline metal oxide particles.<sup>10–12</sup> Many inorganic<sup>13,14</sup> or organic<sup>15,16</sup> methods have been developed to synthesize high quantity spinel powders.<sup>17,18</sup> However, the lack of suitable, consistent, and low cost methods of preparation have limited the abilities of researchers to further explore the applications of high-performance transparent nanoceramics. In this study, nanocrystalline  $\text{MgAl}_2\text{O}_4$  powders

are first synthesized with a low cost high-temperature-calcination method, and transparent  $\text{MgAl}_2\text{O}_4$  nanoceramics have been sintered using these nanocrystalline powders at relatively low temperatures under high pressure.

High purity  $\text{NH}_4\text{Al}(\text{SO}_4)_2 \cdot 12\text{H}_2\text{O}$  and  $\text{MgSO}_4 \cdot 7\text{H}_2\text{O}$ , with a molar ratio of 2:1, were first dissolved into an appropriate amount of de-ionized water in our experiment. The mixed solution held in a quartz vessel was then put into a muffle oven for calcination at 1150 °C for 4 h. Afterwards, nanopowders of  $\text{MgAl}_2\text{O}_4$  can be obtained via screening.<sup>19</sup> The average particle size of the powders is about 20 nm. An appropriate amount of powder was first dry pressed manually under 20 MPa into a small cylinder. The cylinder was then inserted into a cubic pyrophyllite cell which is a pressure-transmitting medium, and assembled to the press-standing piece with other modules including a carbon heater. Sintering of the  $\text{MgAl}_2\text{O}_4$  ceramic was performed in a six-pressure-source cubic anvil device (model DS×800A).<sup>20</sup> The sintering was conducted at 500–700 °C under 2.0–5.0 GPa. First, the pressure was increased and maintained at a preset value. Subsequently, the temperature was increased to the preset value and maintained there for 30 min. When the experiment was completed, the temperature was slowly decreased to room temperature, and then the pressure was gradually reduced. The dimensions of the sintered sample was  $\Phi 12 \times 4 \text{ mm}^2$ . After the sintered samples were polished, their morphologies were observed by scanning electron microscopy (SEM). The average grain size shown in the SEM images was analyzed using the ATOMIC IMAGES 3.1 software. The UV-VIS-IR transmission spectra of the samples were measured with a Perkin-Elmer Lambda 19 spectrometer. The density of the sintered specimens was determined by Archimedes method using a Metler HR51 balance. The nanostructures of the sintered samples were examined by transmission electron microscopy (TEM).

<sup>a)</sup>Electronic mail: lmwang@umich.edu

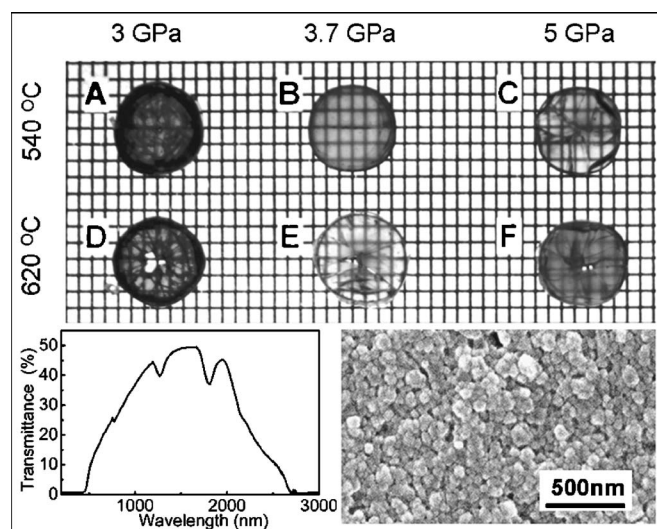


FIG. 1. Appearance of transparent  $\text{MgAl}_2\text{O}_4$  nanoceramics prepared at 540 °C/3 GPa (A), 540 °C/3.7 GPa (B), 540 °C/5 GPa (C), 620 °C/3 GPa (D), 620 °C/3.7 GPa (E), and 620 °C/5 GPa (F), respectively, and a transmission spectrum of sample B and a SEM image of sample E.

All of the samples sintered under 500 °C are opaque. From 540 to 700 °C, the sintered samples are transparent with a light brown color. Above 700 °C, the influence of carbon diffusion becomes significant, resulting in a sharp decrease of transparency. Figure 1 shows the typical appearance of the  $\text{MgAl}_2\text{O}_4$  ceramic specimens prepared at different conditions. At 540 °C, the transparency of samples increases with increasing pressure from 3.0 to 3.7 GPa and 5.0 GPa. At 620 °C, the transparency of samples first increases then decreases with increasing the pressure from 3.0 to 5.0 GPa. The one sample prepared under 3.7 GPa is highly transparent although it has cracked. A transmission spectrum from the sample, without cracks, prepared at 540 °C/3.7 GPa is shown as the insert in the lower-left corner of Fig. 1. In the visible region (400–700 nm), the transmittance increases with increasing wavelength. In the near-middle IR region, the transmittance first increases with the increasing wavelength from 700 to 1400 nm, then saturates from 1400 to 1750 nm. The transmittance at the saturation plateau can reach 50% for the extremely thick sample (4 mm). The transmittance decreases with increasing wavelength from 2000 to 2700 nm. The shape of the transmission spectrum of the samples is the same as that of the conventional micron-grained transparent  $\text{MgAl}_2\text{O}_4$  ceramic. However, the cutoff wavelength in the IR band is at 2700 nm for the nanoceramic, and that of conventional transparent ceramic is at about 6000 nm.<sup>21</sup> Moreover, two absorption peaks emerge at 1300 and 1800 nm, respectively. These peaks have not been observed in conventional transparent ceramics, indicating a unique optical absorption mechanism from nanostructure. It is known that the IR cutoff in transmission is induced by absorption via thermal vibration while that for visible light is induced mainly by electronic transition accompanied by optical absorption in  $\text{MgAl}_2\text{O}_4$  micronceramic. Due to quantum size effect, the transmission spectrum of nanoceramic is blueshifted and becomes narrower, i.e., IR cutoff is shifted from 6000 to 2700 nm. On the basis of the observation of the two absorption peaks induced by  $\text{Al}^{3+}$  ions in oxygen octahedra in  $\text{MgAl}_2\text{O}_4$  powders,<sup>22,23</sup> we believe that  $\text{Al}^{3+}$  ions are also responsible for two absorption peaks

TABLE I. Average grain sizes of ceramics prepared under different conditions.

$\text{MgAl}_2\text{O}_4$ (°C)	2 GPa (nm)	3 GPa (nm)	3.7 GPa (nm)	5 GPa (nm)
540	...	~65	~57	...
620	~80	~70	~61	~50
700	...	~76	...	...

seen in Fig. 1. It is also known that in nanostructures, due to nanoconfinement, the energy levels and energy separations of the impurities states can be enhanced significantly. The energy difference of two peaks shown in Fig. 1 is larger than that observed for micropowder materials.

The insert in the lower-right corner of Fig. 1 is a SEM image of the  $\text{MgAl}_2\text{O}_4$  transparent ceramic prepared at 620 °C/3.7 GPa. The grains are of uniform size. Relating optical property of the ceramics to their morphologies, the uniform grain size seems to be beneficial for improving transparency for the nanoceramic. The average grain sizes based on the SEM images of ceramics prepared at different conditions are shown in Table I. The grain sizes in all samples are less than 100 nm. The average grain size depends on the sintering conditions. At 620 °C, the average grain size decreased from 71 to 50 nm when the pressure was increased from 2.0 to 5.0 GPa. Obviously, the grain growth is restrained under the high pressure.<sup>24</sup> Under 3 GPa, the average grain size increased just slightly with the increasing sintering temperature from 620 to 700 °C.

Figure 2 shows a bright-field TEM and a high-resolution transmission electron microscopy (HRTEM) image of the highly transparent nanoceramic prepared at 620 °C/3.7 GPa. Based on the TEM images, the nanoceramic has a fine-grained, crystalline structure with dense grain boundaries and a few nanosized pores mainly exist in triple junctions of the grains. Figure 3 shows the relationship between the relative density and pressure (a) as well as temperature (b). The relative density of all samples is higher than 97%, in particular, the highly transparent ceramics approaches 99% of the theoretical density. As for conventional micron-grained transparent ceramics, when the relative density of the micron-grained ceramic is lower than 99.5%, it may show a low transparency or even be opaque. It is important to note that the nanopowders prepared by high temperature calcinations are easy to be sintered into dense nanoceramics using low-temperature high-pressure sintering, and the nanoceramic can be highly transparent despite of their lower relative density. The light transmission mechanism for

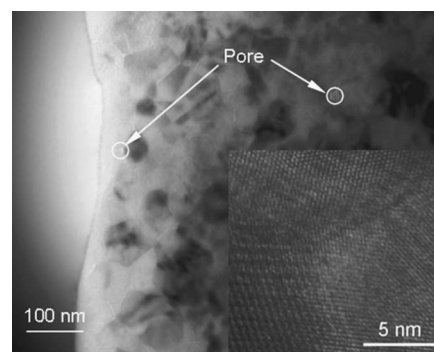


FIG. 2. TEM images of transparent  $\text{MgAl}_2\text{O}_4$  nanoceramics prepared at 620 °C/3.7 GPa.

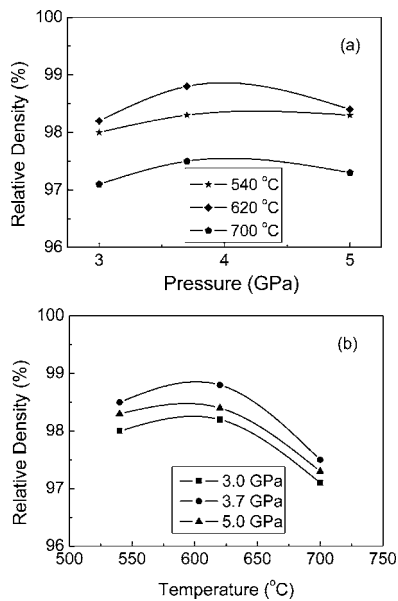


FIG. 3. Relative density of the nanoceramics as a function of sintering pressure (a) and temperature (b), respectively.

the transparent nanoceramics may be different from that for conventional transparent ceramics. Apetz and Bruggen<sup>25</sup> developed a model for light transmission properties of fine-grained, fully dense, polycrystalline Al<sub>2</sub>O<sub>3</sub> ceramic consisting of birefringent crystal based on Rayleigh-Gans-Debye light-scattering theory of geometrical optics. With the model, transmittance ( $T$ ) can be calculated as a function of grain size ( $r$ ), wavelength, and sample thickness. As a result,  $T \propto \exp(-r)$ , indicating the transmittance may increase exponentially with the decreasing grain size in a ceramic. Peelen and Metselaar<sup>26</sup> have calculated the effect of porosity on the transmittance based on Mie scattering theory. Apetz and Bruggen further developed the model so it can be directly applicable to porous polycrystalline materials. When the pore size is less than 10 nm, they reckon, the transmittance can reach the theoretical limit. As a result, high transmittance of polycrystalline ceramics can be achieved by controlling the pore size. For the nanograined polycrystalline ceramic, both lower grain scattering and lower pore scattering must be responsible for the high transparency. Moreover, MgAl<sub>2</sub>O<sub>4</sub> has a cubic crystal structure that does not show birefringence, thus it is not subject to the loss of transmittance due to birefringence. When the relative density of a ceramic is too low (below 98%), the material is opaque regardless of its grain size. The low-temperature high-pressure sintering provides a significant opportunity for preparing highly transparent nanoceramics. When the sintering temperature is increased above 700 °C, or the sintering pressure is increased above 5.0 GPa, carbon diffusion results in a sharp decrease in density that leads to a sharp reduction in transmittance of light.

In summary, transparent MgAl<sub>2</sub>O<sub>4</sub> nanoceramics have been prepared at 540–700 °C/3.0–5.0 GPa. The higher the sintering temperature and pressure are, the greater the densification of sample is. At a same temperature, the higher pressure leads to smaller average grain sizes. Under the constant pressure, the higher temperature results in larger average grain sizes. The relative density of all samples is less than 99%, but some of the samples are highly transparent. The responsible physical mechanism for the high transparency of nanoceramics must be related to the low or negligible light scattering from the nanosized grains and pores. The optimal sintering condition, for highly transparent MgAl<sub>2</sub>O<sub>4</sub> nanoceramic, has been determined to be around 620 °C/3.7 GPa.

This work was supported by NSFC of P.R. China under Grant No. 50272040, Fok Ying Tong Education Foundation under Grant No. 91046, and Youth Science and Technology Foundation of Sichuan Province under Grant 03ZQ026-039. Electron microscopy analysis was conducted at the Electron Microbeam Analysis Laboratory of the University of Michigan. One of the authors (L.W.) acknowledges the support of US NSF NIRT program under Grant No. EAR0403732.

- <sup>1</sup>R. J. Barton, *J. Am. Ceram. Soc.* **54**, 141 (1971).
- <sup>2</sup>P. F. Becher, *Am. Ceram. Soc. Bull.* **56**, 1015 (1977).
- <sup>3</sup>A. F. Dericioglu and Y. Kagawa, *J. Eur. Ceram. Soc.* **23**, 951 (2003).
- <sup>4</sup>M. Barj, J. F. Bocquet, K. Chhor, and C. Pommier, *J. Mater. Sci.* **27**, 2187 (1992).
- <sup>5</sup>G. E. Gazza, *J. Am. Ceram. Soc.* **55**, 172 (1972).
- <sup>6</sup>D. W. Roy, J. L. Hastert, L. E. Coubrough, K. E. Green, and A. Trujillo, U.S. Patent No. 5244849 (14 September 1993).
- <sup>7</sup>M. R. Gallas, A. R. Rosa, T. H. Costa, and J. A. H. da Jornada, *J. Mater. Res.* **12**, 764 (1997).
- <sup>8</sup>M. R. Gallas, B. Hockry, A. Pechenik, and G. J. Piermarino, *J. Am. Ceram. Soc.* **77**, 2107 (1994).
- <sup>9</sup>M. F. Zawrah and A. A. El-Kheshen, *Br. Ceram. Trans.* **101**, 71 (2002).
- <sup>10</sup>L. L. Shaw, Z. G. Yang, and R. M. Ren, *Mater. Sci. Eng., A* **244**, 113 (1998).
- <sup>11</sup>R. N. Das, A. Pathak, and P. Pramanik, *J. Am. Ceram. Soc.* **81**, 3357 (1998).
- <sup>12</sup>A. K. Adak and P. Pramanik, *J. Mater. Sci. Lett.* **17**, 556 (1998).
- <sup>13</sup>M. B. J. Barj, K. Chhor, and C. Pommier, *J. Mater. Sci.* **27**, 2187 (1992).
- <sup>14</sup>D. G. U. Klissurski, *Chem. Mater.* **3**, 1060 (1991).
- <sup>15</sup>P. A. N. Wright, J. M. Thomas, and P. L. Gai-Boyes, *Chem. Mater.* **4**, 1053 (1992).
- <sup>16</sup>T. S. A. Tsumura and M. Inagaki, *J. Mater. Chem.* **3**, 995 (1993).
- <sup>17</sup>E. P. Pyskhewitch, *Bull. Mater. Sci.* **19**, 957 (1996).
- <sup>18</sup>O. H. N. Varnier, A. Larbot, P. Bergez, and L. C. Charpin, *Mater. Res. Bull.* **29**, 479 (1994).
- <sup>19</sup>H. B. Li, D. X. Wu, and L. B. Lin, *Bull. Chin. Ceram. Soc.* **22**, 304 (1993).
- <sup>20</sup>X. J. Luo, Q. Liu, and L. Y. Ding, *J. Mater. Sci. Lett.* **16**, 1005 (1997).
- <sup>21</sup>D. W. Roy, *Proc. SPIE* **297**, 13 (1981).
- <sup>22</sup>J. Preudhomme and P. Tarte, *Spectrochim. Acta, Part A* **27**, 961 (1971); **27**, 851 (1971); **27**, 1817 (1971).
- <sup>23</sup>C. Pommier, K. Chhor, J. F. Bocquet, and M. Barj, *Mater. Res. Bull.* **25**, 213 (1990).
- <sup>24</sup>S. C. Liao, Y. J. Chen, B. H. Kear, and W. E. Mayo, *Nanostruct. Mater.* **10**, 1063 (1998).
- <sup>25</sup>R. Apetz and M. P. B. Bruggen, *J. Am. Ceram. Soc.* **86**, 480 (2003).
- <sup>26</sup>J. G. J. Peelen and R. Metselaar, *J. Appl. Phys.* **45**, 216 (1974).